INFLUENCE OF BINDER
ON THE MECHANICAL PROPERTIES AND THE PERMEABILITY OF
A NON-CRIMP CARBON FABRIC PREFORM

M. Dickert[*], G. Ziegmann

Institute of Polymer Materials and Plastics Engineering, Clausthal University of Technology
* corresponding author: matthias.dickert@tu-clausthal.de

Keywords: Preform, Binder, Mechanical Properties, Permeability

Abstract
Preforms have been produced from a non-crimp fabric using different press parameters and binder types. High press temperatures and long pressing times first lead to a binder particle deformation and then to capillary flow of the binder between the filaments. This deformation / flow affects the preform's peel strength and bending properties as well as its permeability. Increasing amounts of binder lead to higher peel strengths; the relation, however, is not linear. In contrast, bending strengths exhibit a linear relation. In the case of peel strength, an optimum can be observed for different press times and different temperatures which does not occur with three-point-bending. Permeability is also influenced in an unanticipated manner. In one fabric we find both a permeability increase as well as a decrease depending on the preform parameters and binder types.

1. Introduction

Binders or tackifiers are thermoplastic or thermoset materials which are used to bond individual fabric layers to each other thereby producing a preform of a desired geometry. Commonly, binder is applied to a fabric as powder or as veil. It then is activated by infrared radiation to stick to the textile. Another typical technique is to spray a binder solution directly onto the fabric. In order to obtain a preform, the bindered textile is cut, stacked and shaped before the binder is activated again.

The production of FRP parts involves several steps: 1) preforming, 2) resin infusion, 3) resin cure, 4) cured part. Binder influences all these stages [1-6]. Often, this happens in an undesired way. In spite of that, little attention was paid to the question: what is the minimum binder content? Few authors varied binder contents or activation parameters and systematically studied the resulting effects on preform properties [7-12]. This, however, is necessary to answer the question raised above and to find a suitable set of activation parameters. It is likely that these parameters are a key enabler for further reduction of binder content in preforms which is the reason for their thorough investigation in this work.

2. Materials and Methods

2.1 Preform Preparation

Table 1 lists all materials used. EPR5390 is a standard binder in FRP applications and has therefore been chosen to be used in this study. Other binders are for comparison only. S37CX also is a standard textile.

Type	Name	Manufacturer	Description
Binder	EPR5390	Momentive	Epoxy powder, T_g: 61 °C, $D_{50}(Q_3)$: 106 µm, sieve spacing: 100 µm
Binder	PA1401	Spunfab	Co-Polyamid veil, T_g: 95 °C, Areal weight: 6 g/m²
Binder	Vinnex LL2319 A9133	Wacker	Acrylate Styrene Co-Polymer powder, T_g: 63 °C, $D_{50}(Q_3)$: 82 µm, sieve spacing: 63 µm
Fabric	S37CX000 0301 01400 264000	Saertex	Carbon, 0/90° Biaxial, non-crimp, Areal weight: 308 g/m²

Table 1: Used materials

Binder is applied onto the textile using a sieve and a scale. It is placed between two adjacent layers of textile. The applied amount is determined based on the areal weight of the layer it is applied to. The preform is made from six plies and hence its binder content is slightly lower, because only five interlayers can be found in a stack. However, in this work binder content refers to the ratio of binder weight over ply weight. The stack is then hot-pressed with the pressing parameters being varied according to Table 2. Preform thickness is controlled by distance plates. The base parameters for this study are 90 °C pressing temperature, 1 min pressing time, 2 wt.% binder content, and EPR5390 binder type. A parameter study covering the preform parameters is conducted for EPR5390 with only one of the parameters changed at a time. For permeability measurements, the two other binder types are used for comparison only. No comparable parameter study is conducted for these binders.

Test specimen	# of fabric layers	Binder content in wt. %	Press temperature in °C	Press duration in s	Sample size in mm x mm	Preform thickness in mm
T-peel	2	1, 2, 3, 4, 5, 10	90	1	250 x 25	1
T-peel	2	2	70, 80, 90, 100, 110, 130, 160	1	250 x 25	1
T-peel	2	2	90	30, 60, 120, 220, 300, 600, 1000, 2400, 3600	250 x 25	1
3-point bending	4	1, 2, 3, 4, 5, 10, 100	90	1	100 x 25	2
3-point bending	4	2	60, 70, 80, 90, 100, 110, 130	1	100 x 25	2
3-point bending	4	2	90	15, 30, 60, 120, 220, 300, 600, 1000	100 x 25	2

Table 2: EPR5390 activation parameters

T-Peel Test

A piece of foil is placed between the two layers at one side in order to locally prevent their bonding. Samples of 250 mm x 25 mm are cut from the pressed preform. The loose ends are fixed in the clamps of a universal testing machine (Zwick, BZ100/TL3A) operated in tensile mode. A 20 N load cell is used to measure the peel force under a constant cross head speed of 50 mm/min. The tear length is 200 mm. Force is recorded depending on crosshead position. Peel force is determined as mean value of force over 50 mm – 200 mm tear length.

Three-Point-Bending Test

Samples of 100 mm x 25 mm are cut from the pressed preform. The sample is then placed in the text fixture with a support span of 60 mm and a loading radius of 5 mm. The universal testing machine mentioned before is set to compression mode and the force needed to maintain a constant movement of 50 mm/min is recorded along with the corresponding position using a 20 N load cell. Bending modulus is calculated from this data. Maximum bending force (R_m) and the deflection apparent at this point are also determined.

Permeability Measurements

Permeability is measured using an apparatus devised by the authors, which allows for an optical tracking of the flow front. The textile is placed between a glass plate and a steel plate. To avoid deflection of the cavity, the steel plate and the glass plate are both supported by a block of cross beams with a height of 15 cm each. These blocks are bolted together to achieve the compaction of the textile. The height of the cavity is determined by a set of spacers, which are inserted around the textile. However, the height of the cavity is also measured ex-post using waxen pellets that are compacted along with the textile. This allows for determining the actual height and noticing possible deflections of the cavity.

The injection fluid is a vegetable oil of a known, temperature-dependent viscosity of about 100 mPa·s. The injection pressure is adjusted using a pressure control valve. Race tracking is prevented in this setup by a special concept that allows proper sealing of the edges of the textile once the textile has been compacted to its final thickness. The advance of the flow front is captured by the use of a camera operating in continuous shooting mode. The obtained images are then evaluated using semi-automated software. Permeability is calculated according to Darcy's Law.

Although both layers are made from the same type of fiber at the same fiber volume content (FVC), 2D permeability experiments show a flow ellipse tilted by 16°. The reason for this is that stitching is not symmetric for the two layers within the chosen biaxial textile. In this study 1D experiments are conducted – hence a corresponding preform rotation is necessary. Test parameters are presented in Table 3.

Description	Binder type	Binder content	Preforming parameters	FVC
Lay-up 1	EPR5390	0, 2, 4, 6 wt.%	1 min, 90 °C, 3.0 mm	40.7 %
Lay-up 2	PA1401	0, 2 wt.%	1 min, 120 °C, 3.0 mm	40.7 %
Lay-up 3	A9133	0, 2 wt.%	1 min, 160 °C, 3.0 mm	40.7 %

Table 3: Used lay-ups for permeability measurements

Results and Discussion

Hot-pressed preforms were debonded and subjected to light microscopy. Pictures of the interlayer reveal the general concept of binder behavior during activation. Figure 1 shows how for a given pressing time (1 min) and increasing pressing temperatures the binder deforms (90 °C), melts (110 °C), and finally flows between filaments (160 °C) until no binder can be found on the roving surface. Naturally, for other fiber types, pressing distances, or pressing durations the findings will differ.
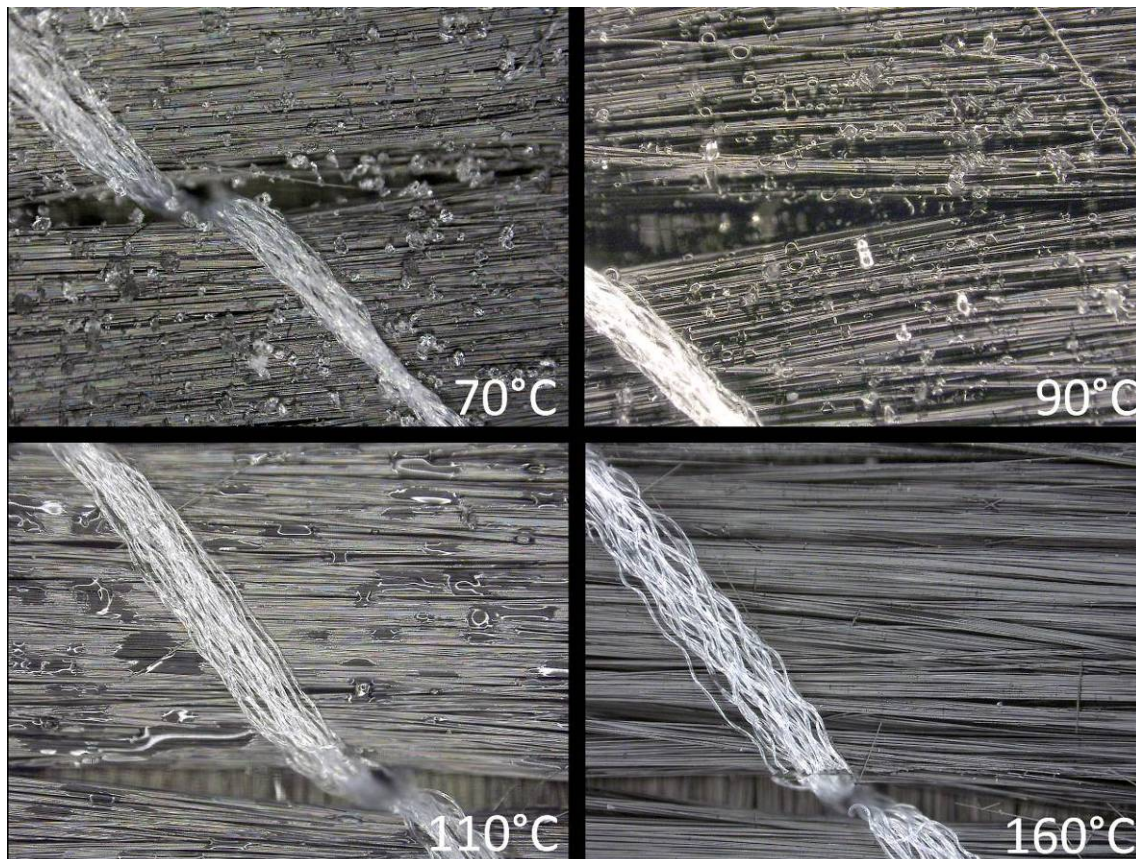
Fig. 1: Different pressing temperatures applied to EPR5390 for 1 min

A distinct interlayer can be found (Fig. 2) when examining preforms produced with different binder contents and activated at a low (90 °C) pressing temperature. The area coverage increases with increasing binder content. At 4 wt.% binder content, binder particles start to form agglomerations which for 5 wt.% become very pronounced. At 10 wt.% hardly any uncovered roving surface is visible. Also, the binder distributes evenly on the roving surface. While some particles fall into the space between two rovings, a seemingly similar amount with respect to the area is located on the roving surface. An interesting feature can be found in the 5 wt.% picture: no binder at all is visible underneath the stitching yarn.

T-peel test results are in accordance with microscope observations. Figure 3a shows an increase of peel force with increasing binder contents. An almost linear trend holds from 0 – 3 wt.%. Binder contents above 4 wt.% do not yield significant increases in peel force – a plateau is reached. This corresponds with the roving coverage found in Figure 2 where first an increase is visible and beginning at 4 wt.% similar coverage is seen with increasing binder amounts.
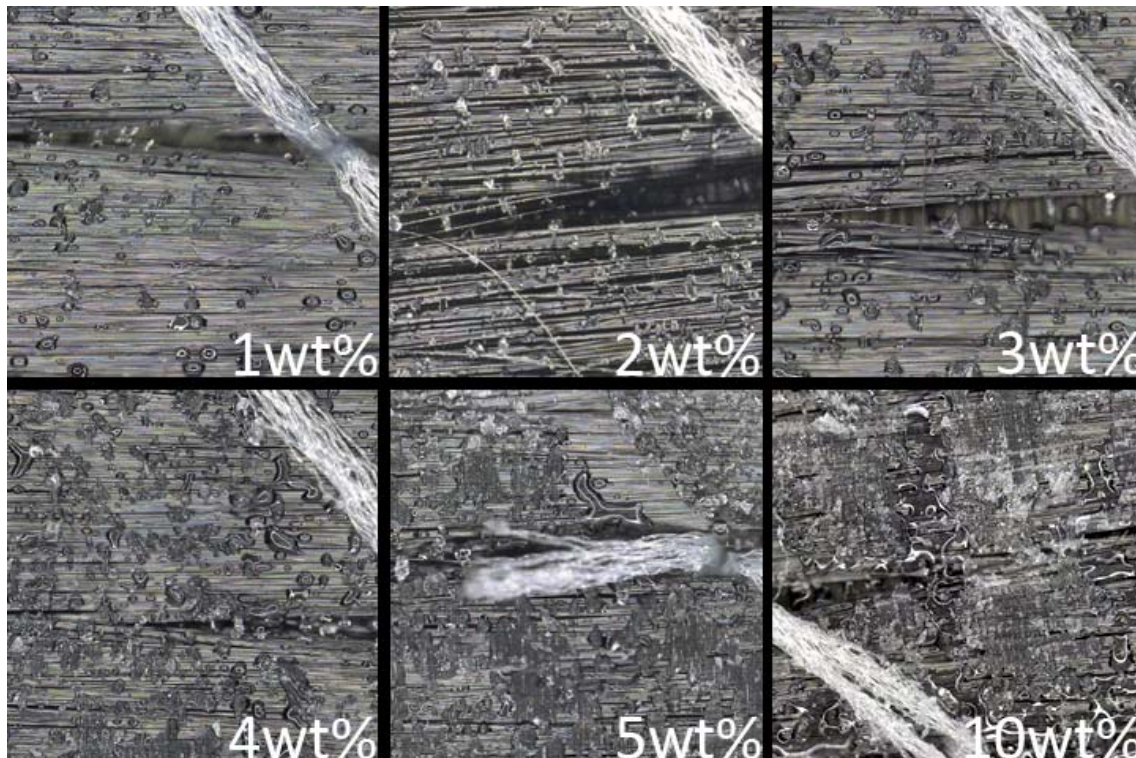
Fig. 2: Different EPR5390 contents pressed for 1 min at 90 °C

Experiments with varying pressing temperatures (Fig. 3b) show a peel force curve with a maximum at about 90 °C. At this temperature, traces of particle softening and beginning flow can be found. While binder particles activated at 70 °C exhibit sharp edges, binder topology is much smoother at 90 °C. This coincides with the maximum peel force. At 110 °C some binder has already flown between filaments and the resulting peel force is smaller. Preforms produced at 160 °C did not bond at all so testing was not possible and the peel force assumed to be zero.
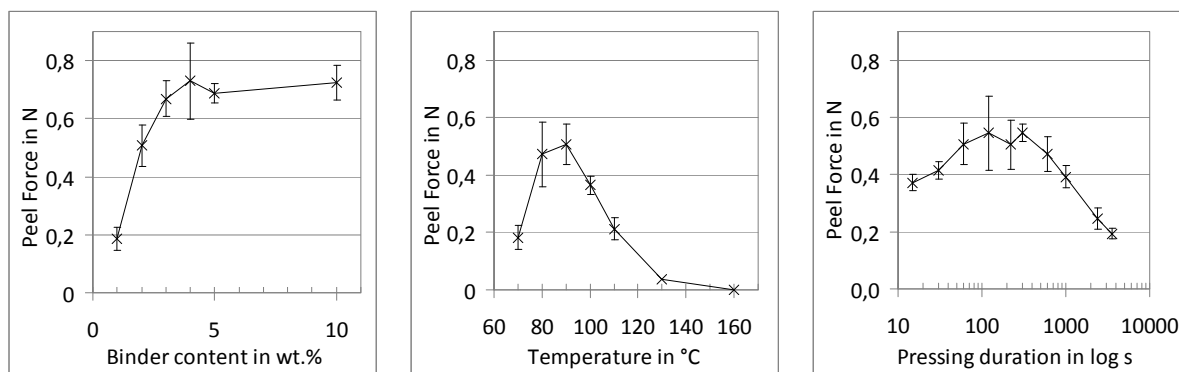

Fig. 3 a – c: T-peel test results

Different pressing durations at 90 °C pressing temperature (Fig. 3c) also show a peel force curve with a maximum which can be found for about 90 – 220 s. The peel force curve's progression over time can be attributed to the first increasing and then decreasing size of the contact area between binder and filaments due to particle deformation or flow.

Peel force strongly depends on the binder amount available in the interlayer and the roving area covered. Adding binder increases both parameters. At a certain threshold the entire

roving area is covered, therefore, the further addition of binder has no effect on the resulting peel force.

Binder is first softened by a temperature increase and finally melts. In the softened state, press forces mold binder particles into the roving's first layer of filaments thus increasing the area in which adhesive forces can act. Higher temperatures lead to a viscosity decrease; consequently, more binder migrates into the inter-filament spaces during the activation cycle. This might transfer some load bearing towards cohesive effects since individual filaments can be surrounded by binder and form fit is important in that case. However, considering the particle size, the fiber orientation and the resulting capillary forces, the penetration depth can be assumed to be small. Binder particles rather spread out on the roving surface. Particle volume thus decreases and its load bearing cross section with it. For this reason peel force decreases at elevated temperatures. At very high temperatures, i.e. low viscosities, binder completely migrates into the roving reducing the amount of binder in the interlayer to almost zero. Exchanging time for temperature, similar results can be expected. Although, the time scale covered in this study is too short to obtain a peel force of zero, the general trend resembles the results for varying temperatures.

Results of 3-point bending tests support the concept of binder migration and a corresponding change in mechanical behavior of the preform. Figures 4 – 5 present the respective results. Bending modulus (a), maximum force (R_m), (b), and the deflection reached at maximum force (c) are shown.
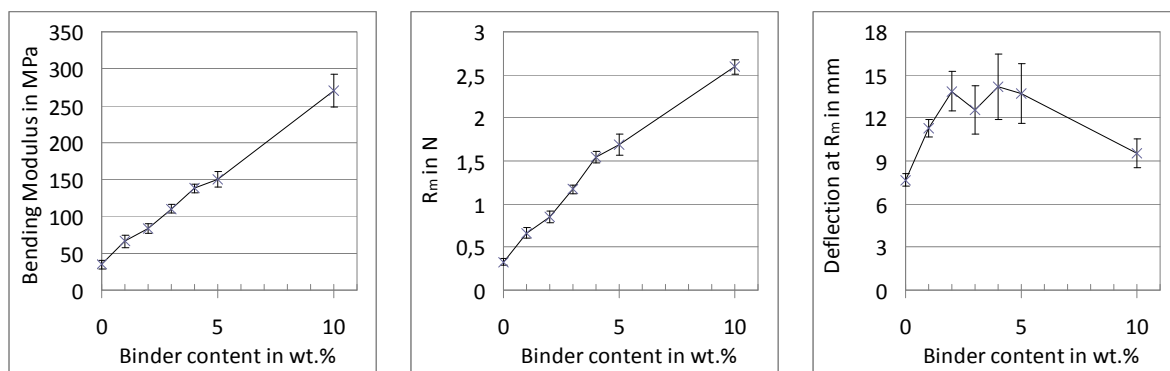

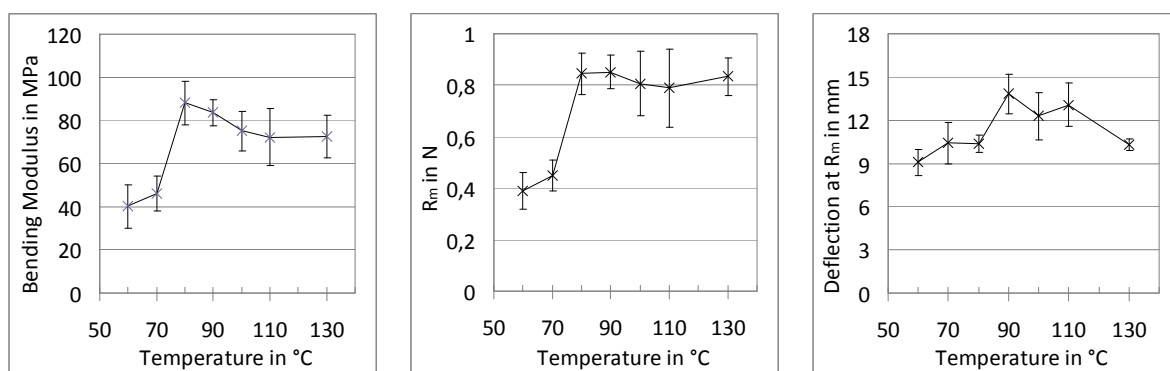Fig. 4 a – c: Results of 3-point bending tests with varying binder contents

Fig. 5 a – c: Results of 3-point bending tests with varying pressing temperatures

For a range of 0 – 10 wt.% binder content, a linear relation of binder content and bending modulus is observed. The maximum force also increases linearly, but the deflection at R_m decreases for binder contents higher than 5 wt.% (Fig. 4 a – c). By adding more binder a

greater number of filaments are bonded at a greater number of individual bonding points. The mean free path between two supports decreases and thus more load is transferred into the fibers and the preform becomes stiffer. At some point a state of binder reinforced fibers is reached and the "preform" properties should be calculable by rule of mixture. This thought helps in understanding the increase of R_m itself as well as the decrease of deflection at R_m.

Test results for varying temperatures show a behavior of two states. At low temperatures, bending modulus and maximum force are low. At a certain transition temperature values change to a different level. Deflection however remains almost constant (Fig. 5 a – c Temperature). In the range of low temperatures, binder particles are merely pressed and adhesion is either bad or the only force bonding filaments. In the higher temperature range, binder flows between filaments and either adhesion area increases significantly or another type of bonding force, i.e. cohesion, acts additionally. From peel experiments it is known that almost the entire binder has flown into the inter-filament spaces. If the same is assumed for 3-point bending test samples (FVC during pressing is kept constant for both sample types), it can be concluded that binder location has an entirely different effect on mechanical properties. Binder only needs to be inside the preform somewhere in order to effectively stiffen it against bending. As long as it is activated at a temperature high enough, the positioning – in the interlayer or inside the roving – does not influence the properties tested. This can readily be explained with the stiffening mechanism itself. Filaments are pliable as long as they can move freely. If their freedom of movement is hindered, the preform stiffens. This happens for two filaments of the same roving bonded together in the same way as for two filaments of different rovings hence a complete migration of binder into the roving does not alter that mechanism. Figure 6 summarizes these thoughts and helps in understanding the different results of 3-point bending tests and peel tests.
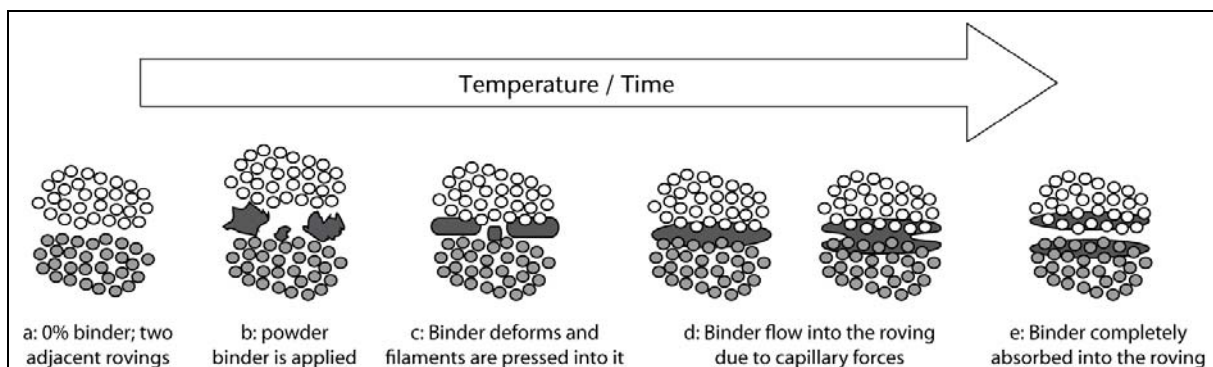

Fig. 6: Concept of binder movement

It is obvious that binder influences preform porosity and porosity distribution. Both parameters take part in determining permeability. Therefore, experiments were conducted with the aim of characterizing the permeability of preforms which were processed at conditions where the binder stayed in the interlayer.

Preliminary results show an influence of binder that exceeds a relationship between its mere content and permeability (Fig. 7). Three different binder types at the same binder content yield different permeabilities. Permeability in Lay-up 1 is first increased and then decreases again with increasing binder content. This is attributed to a spacer effect of binder particles which are activated with parameters that allow for little flow only (cp. Table 3). At low binder contents new flow channels are created in the vicinity of a binder particle. For higher binder contents they are gradually clogged and permeability decreases.
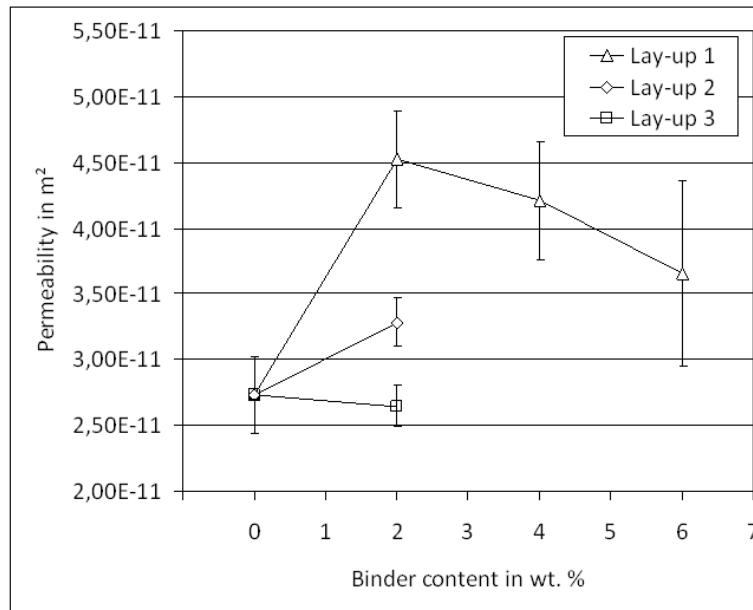
Fig. 7: Results of permeability tests with different binder types and contents

References

[1] Chen J., Backes D., Jayaraman K., Dynamics of Binder Displacement in Liquid Molding. *Polymer Composites*, **17**, 23-33, (1996).

[2] Hillermeier R.W., Seferis J.C., Interlayer toughening of resin transfer molding composites. *Composites Part A*, **32**, 721-729, (2001).

[3] Brody J.C., Gillespie J.W., The Effect of a Thermoplastic Polyester Preform Binder on Vinyl Ester Resin. *Journal of Thermoplastic Composite Materials*, **18**, 157-179, (2005).

[4] Depase E.P., Hayes B.S., Seferis J.C., *Interlayer toughened VARTM composites using preformed particle toughened tackifiers*. Proceedings of the 33rd International SAMPE Technical Conference, USA, (2001)

[5] Knight J.C., Backes D., Jayaraman K., Consolidation and Relaxation Behavior of Continuous Strand Random Glass Mats With Thermoplastic Binders. *Polymer Composites*, **17**, 451-457, (1996)

[6] Tsotsis T.K., Interlayer Toughening of Composite Materials, Polymer Composites, 30, 70-86, (2009)

[7] Tanoglu M., Seyhan A. T., Compressive mechanical behaviour of E-glass/polyester composite laminates tailored with a thermoplastic preforming binder. *Materials Science and Engineering A*, **363**, 335-344, (2003).

[8] Brody J.C., Gillespie J.W., Reactive and Non-reactive Binders in Glass/Vinyl Ester Composites. *Polymer Composites*, **26**, 377-387, (2005).

[9] Shih C.H., Liu Q., Lee L.J., Vacuum-Assisted Resin Transfer Molding Using Tackified Fiber Preforms. *Polymer Composites*, **22**, 721-729, (2001).

[10] Shih C.H., Lee L.J., Tackification of Textile Fiber Preforms in Resin Transfer Molding. *Journal of Composite Materials*, **35**, 1954-1981, (2001).

[11] Rohatgi V., Lee L.J., Moldability of Tackified Fiber Preforms in Liquid Composite Molding. *Journal of Composite Materials*, **31**, 720-744, (1997).

[12] Estrada G., Vieux-Pernon C., Advani S.G., Experimental Characterization of the Influence of Tackifier Material on Preform Permeability. *Journal of Composite Materials*, **36**, 2297-2310, (2002).